J Mater Sci (2008) 43:4391–4398
DOI 10.1007/s10853-007-2437-5

Characterization of long fiber thermoplastic/metal laminates

R. R. Kulkarni · K. K. Chawla · U. K. Vaidya · M. C. Koopman · A. W. Eberhardt

Received: 1 November 2007 / Accepted: 28 December 2007 / Published online: 18 April 2008

Abstract Long fiber thermoplastic (LFT) composite/metal laminate (LML) is a hybrid composite consisting of alternate layers of metals such as aluminum and an LFT composite, which combines advantages from both the constituents. The LFT/Al laminates (LMLs) were processed by compression molding and were characterized for their Young's modulus, mechanical strength, and low-velocity impact (LVI) properties. The average values of specific elastic modulus and specific tensile strength were approximately 20 GPa/(gcm^{-3}) and 108.5 MPa/(gcm^{-3}), respectively. Failure mechanisms included delamination between LFT composite and Al, fiber fracture and pullout in LFT composite, and shear fracture of aluminum and LFT composite layers. Rule-of-mixtures (ROM) predictions of laminate properties in tension compared well with the experimental values. Specific perforation energy of the laminates determined by LVI tests was 7.58 J/(kgm^{-2}), which is significantly greater than that of the LFT composite alone, 1.72 J/(kgm^{-2}). Overall, the LML showed significant improvement in the properties as compared to the LFT composite.

R. R. Kulkarni (✉) · K. K. Chawla · U. K. Vaidya · M. C. Koopman
Department of Materials Science and Engineering, The University of Alabama at Birmingham, 1530 3rd Ave S, BEC 254, Birmingham, AL 35294, USA
e-mail: rrkulkarni@gmail.com

A. W. Eberhardt
Department of Biomedical Engineering, The University of Alabama at Birmingham, 1530 3rd Ave S, Hoehn 368A, Birmingham, AL 35294, USA

Introduction

Long fiber thermoplastic (LFT) composite/metal laminate (LML) is a *hybrid* composite consisting of alternate layers of LFT composite and metal such as aluminum. LFT composites constitute a family of composites, wherein a thermoplastic matrix such as polypropylene, nylon, or polyurethane, etc. is reinforced with discontinuous fibers (fiber lengths between 10 and 50 mm). The major advantages of LFT composites are that their low cost and they can be processed using traditional plastic molding operations such as compression molding, extrusion, and injection molding [1, 2].

There are several types of hybrid composite materials. An important example of a hybrid composite are the so-called fiber metal laminates (FMLs), which were developed as an aerospace material; FMLs consist of alternate layers of metal sheet and polymer matrix composites (PMC) reinforced with continuous fibers. The polymer used is generally a thermoset resin such as epoxy. FMLs have advantages such as high-specific strength, good fatigue resistance, high-damage tolerance capabilities, and good formability and machinability [3–8]. New generation FMLs are being developed, which consist of a thermoplastic matrix in the PMC layer instead of thermoset. Thermoset matrices are brittle and have low-fracture toughness values; also, the processing time for the laminates involving thermosets is long. Thermoplastics, on the other hand, have high toughness, short processing times, and are more environmentally friendly because of their recyclability [9, 10]. As an example, consider the FML system based on a thermoplastic composite consisting of alternate layers of titanium (Ti) and glass fiber reinforced polyetherimide (GF/PEI) [9]. This FML system based on PEI can be used for high temperature applications because

of its higher glass transition temperature compared to poly ether ether ketone (PEEK). In another study [10, 15], the impact resistance of polypropylene based FMLs was found to be higher than that of thermoset based FMLs.

Some other examples of hybrid composites used in the automotive industries are SMCs (sheet molding compounds reinforced with continuous fibers), GMTex (glass mat thermoplastics reinforced with woven fabrics), and E-LFT (LFT composite reinforced with continuous fibers, also called as tailored LFT). In all the above examples, the properties of the baseline materials (such as SMC, GMT, and LFT, which contain discontinuous fibers, chopped or long) are enhanced by reinforcing them with the continuous fibers [11–14]. The objective of this work was to characterize a new hybrid material called LML, which combines an LFT composite with a metal such as aluminum. The LML combines advantages from both of its constituents and hence can have properties like high-specific modulus and strength, damage tolerant, vibration and sound damping, formability and machinability, etc. Potential applications of LMLs are in automotive, military, and construction sectors.

Materials and experimental procedures

Long fiber thermoplastic composite/metal laminates were processed using nylon 66 LFT (12 mm long pellets and 23 volume % fibers) and aluminum alloy 2024. The laminates were processed by compression molding. The laminates were molded in 2/1 configuration, which consisted of one layer of LFT composite between two aluminum plies. Mechanical behavior of the laminates was characterized by tensile, three-point bend, and low-velocity impact tests.

Tensile testing

Tensile testing was performed on rectangular specimens of dimensions 15 × 140 × 1.4 mm. The testing was done on a TC-55 Instron servohydraulic test frame. The crosshead velocity was 2 mm/min. A clip-on extensometer was used to measure the displacement of the gage length, which allowed values of Young's modulus of the laminates to be obtained. After failure, the fracture surfaces of samples were observed in a scanning electron microscope.

Three-point bend tests

Three-point bend tests were done on a T-5000 Satec electromechanical test frame. Load versus displacement plots were obtained for each sample. The load-displacement plots were then converted to stress-apparent strain (obtained form the crosshead displacement) curves. Maximum flexure strength (σ_{max}) values were calculated based on the peak load value in the load versus displacement curves using the following relationship.

$$\sigma_{max} = \frac{3P_{max}S}{2Bd^2} \quad (1)$$

where P_{max} is the maximum load and S, B, and d are span length, breadth, and thickness of the sample, respectively.

Short beam test

Short beam tests were done to estimate the interlaminar shear strength (ILSS) of the LML samples. The test was done on two sets of samples, one with interfacial surface roughness corresponding to the as-received condition of the metal and the other sand blasted to increase the surface roughness. The samples were cut according to ASTM standard D2344 from a plate of 2/1 configuration. Load versus displacement plots were obtained from the three-point bend tests and the ILSS was calculated from the following expression:

$$\sigma_{ILSS} = \frac{3P_{max}}{4Bd} \quad (2)$$

where P_{max} is the maximum load, B is the breadth, and d is the thickness of the sample.

Low-velocity impact test

Low-velocity impact (LVI) tests on LMLs and LFT composites were done using a Dynatup 8250 drop weight impact testing machine. The impact tests were carried out on 2/1 laminates using 6.67 kg hemispherical impactor of 19.5 mm diameter. The energy of impact was varied by changing the release height of the impactor. A rectangular fixture having an opening of 75 × 75 mm was used to hold the samples. Square samples of 100 cm^2 were held between two aluminum plates of the fixture. Before impact, weight of each sample was measured. The mass was divided by the area of the square plate to obtain an areal density (mass/area). Samples were tested in successive incremental energies until full perforation. Specific perforation energy (or specific perforation resistance) of LML and LFT composite samples were determined by normalizing the absorbed energy values with their respective areal densities. Similarly, specific peak load was obtained by normalizing the peak load by areal density.

Results and discussion

Tensile testing

Tensile stress–strain curves of the LFT composite/aluminum laminate and LFT composite are shown in Fig. 1. The

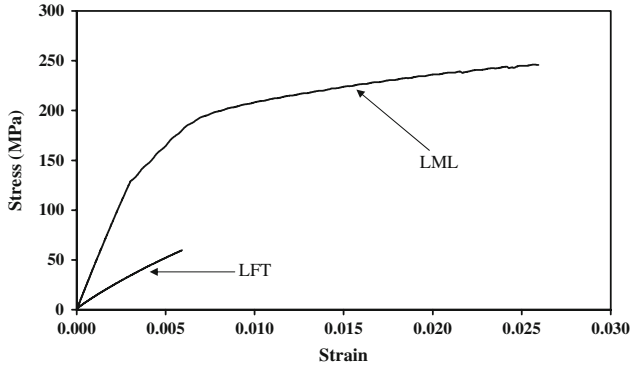

Fig. 1 Tensile stress versus strain curves of LFT composite and LML. Note the nonlinear behavior of an LML and improvement in the properties over an LFT composite

curve for the LFT is practically linear until failure. The LML, however, showed a nonlinear behavior. The nonlinear behavior came mainly from the plastic deformation of the aluminum plies. Examination in a scanning electron microscope showed delaminations between the plies of the laminate, see Fig. 2. During the tensile loading of the LML, LFT composite failed first because of its low strain to failure. Within the LFT composite, various failure mechanisms were observed, including: nylon 66 matrix cracking, fiber/matrix interface debonding, fiber fracture, and pullout, Fig. 3. After the failure of the LFT composite, the load was taken by aluminum plies till the final failure of the LML by delamination at the LFT composite/aluminum interface and fracture of aluminum plies.

The average Young's modulus value of five samples determined was approximately 44.8 ± 3.4 GPa. The average tensile strength of the laminate was found to be 244 ± 5.6 MPa. The average values of specific modulus and strength of the LML were 20 GPa/(gcm^{-3}) and 108.5 MPa/(gcm^{-3}), respectively. There was a significant improvement in the modulus and the tensile strength of the

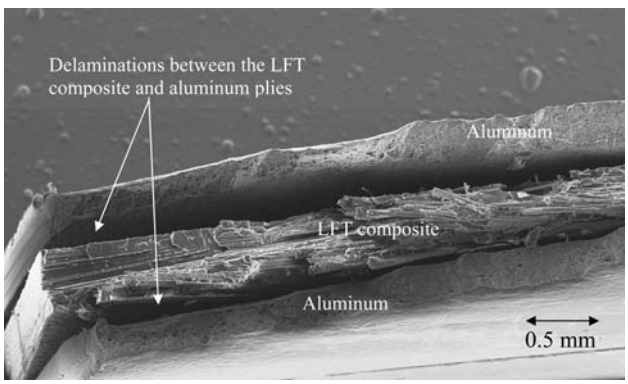

Fig. 2 Failed section of an LML in a tension test showing delaminations between the plies. Note the extensive necking and ductile failure in the aluminum layers

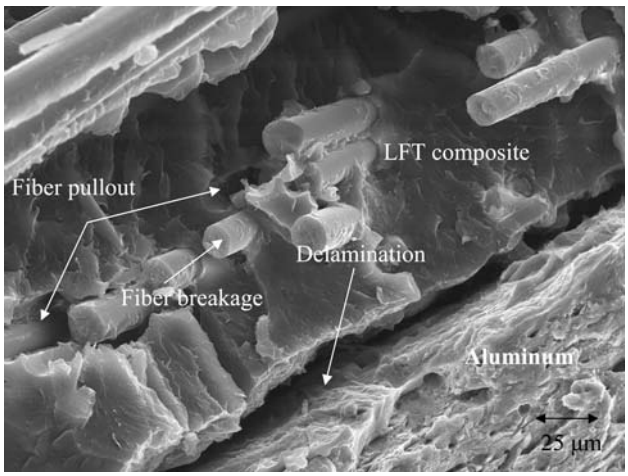

Fig. 3 Fracture surface of the LFT composite showing fiber breakage and pullout. Aluminum fracture surface can also be seen

LML compared to that of the LFT composite. Monolithic aluminum was tested for comparison purpose and its average values of specific modulus and specific strength were 25 GPa/(gcm^{-3}) and 157 MPa/(gcm^{-3}), respectively. Laminate properties were dominated by aluminum.

Rule-of-mixtures (ROM), based on volume fraction of the metal and composite layers in the laminate, was used to predict the laminate properties such as density, Young's modulus, and tensile strength of the laminate [2, 5]. In this case, the LFT composite was considered as one homogeneous isotropic material and the properties were derived by experimental testing and not by applying ROM to their constituents' properties viz. glass fibers and nylon 66 matrix. The volume fraction of aluminum layers (V_{Al}) was calculated as follows [12]:

$$V_{Al} = \frac{\Sigma_1^p t_{Al}}{t_{LML}} \tag{3}$$

where t_{Al} is the thickness of metal layer, p is the number of metal layers, and t_{LML} is the total thickness of the laminate. From this expression, the V_{Al} for our laminate was calculated to be 0.57.

The density of a composite is given by the ROM [2]. The expression for the density of the laminate (ρ_{LML}) can be written as:

$$\rho_{LML} = \rho_{Al} V_{Al} + \rho_{LFT}(1 - V_{Al}) \tag{4}$$

where ρ_{Al} and ρ_{LFT} are density of the aluminum alloy and the LFT composite, respectively. The calculated density value was 2,260 kg/m^3, which agrees well with the experimentally determined value of 2,250 kg/m^3. The difference may be due to a small amount of porosity in the LFT.

In a similar way, to calculate the Young's modulus (E_{LML}) and tensile strength (σ_{LML}, at a particular value of strain) of the laminate following expressions were used:

$$E_{\mathrm{LML}} = E_{\mathrm{Al}} V_{\mathrm{Al}} + E_{\mathrm{LFT}}(1 - V_{\mathrm{Al}}) \quad (5)$$

$$\sigma_{\mathrm{LML}} = \sigma'_{\mathrm{Al}} V_{\mathrm{Al}} + \sigma'_{\mathrm{LFT}}(1 - V_{\mathrm{Al}}) \quad (6)$$

where E_{Al} and E_{LFT} are the Young's moduli of the aluminum and the LFT composite, respectively, σ'_{Al} and σ'_{LFT} are tensile strengths of the aluminum and the LFT composite at a particular value of strain.

The Young's modulus of the LML calculated from Eq. 5 was 44.35 GPa, which compares well with the experimental value of 44.8 GPa. The tensile strength values of the LML at a strain value 0.005 from the ROM and experiment were 183 MPa and 165 MPa, respectively and the discrepancy in the strength values between ROM and experiment is likely due to two reasons: (1) reduction in the strength of the aluminum alloy 2024 after processing of the laminate and (2) because of variation in the strength of the LFT composite because of misorientation of discontinuous fibers. High strength in the aluminum 2024 stems from interaction between dislocations and the finely dispersed precipitates [15]. During the processing of the laminate, the aluminum plies go through a heating and cooling cycle (from about 300 °C to room temperature), which is likely to cause overaging of the alloy and hence coarsening of the finely dispersed precipitates and a reduction in strength. These coarse precipitates are not as effective as the fine precipitates in impeding the dislocation movement and hence a lower strengthening effect leading to a decrease in overall strength of the aluminum alloy occurs. In one study, it was found that the reduction in the strength values could be as large as 20% when the aluminum alloy 2024 was heated to 285 °C [16]. Taking into account the reduction in strength of aluminum only (ignoring the fiber misorientation), the ROM and experimental values of strengths are in a reasonable agreement. Predicted properties of the LML from the ROM and experimental values are summarized in the Table 1.

Three-point bend tests

Three-point bend tests also showed nonlinear behavior of the LML due to plastic yielding of aluminum plies, see Fig. 4. The failure of the laminate was mainly by partial

Table 1 Comparison of the ROM and experimental properties of the laminate

Property	Rule-of-mixtures value	Experimental value
Density (kg/m^3)	2250	2260
Young's modulus (GPa)	44.35	44.8
Specific modulus (GPa/gcm^{-3})	19.70	20.0
Tensile strength at 0.5 % strain (MPa)	152	165

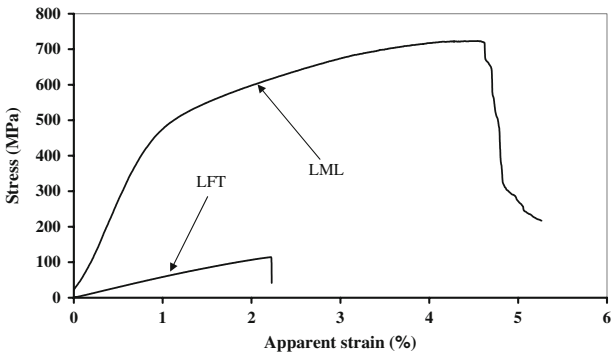

Fig. 4 Stress versus apparent strain plot showing nonlinear behavior of the LML in a three-point bend test

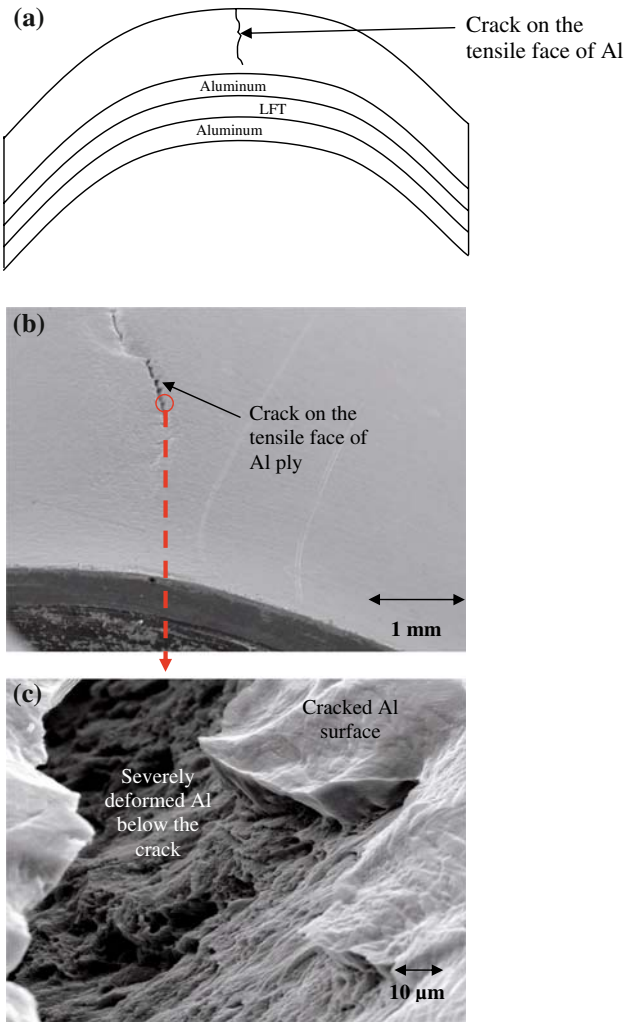

Fig. 5 Failed LML specimen in a three-point bend test. (**a**) Schematic of a deformed laminate showing crack on the tensile side of the aluminum ply. (**b**) SEM picture of a crack on the tensile side of the aluminum ply in the laminate. (**c**) Higher magnification of the cracked surface in the aluminum ply. The portion of aluminum ply below the crack is severely deformed but uncracked

cracking of the aluminum ply on the tensile side of the sample, Fig. 5. No debonding was observed between the plies of the laminate, Fig. 6. The LFT layer in the middle and the top Al layer is in tension while the bottom one is in compression. Aluminum layer did not crack. The maximum flexure strength of the laminate was calculated based on the peak load reached in the flexure test. The LML showed significantly higher peak stress and strain to failure than that of LFT composite alone. The average maximum flexure stress of five LML samples was 683 MPa. The average maximum flexure stress values of the LFT composite in three-point bend test was 160 MPa. Unlike the laminate, the LFT composite failed in a brittle manner. Thus, the laminate showed improvement in flexure strength and damage tolerance.

Flexural strength of the laminate was mainly dominated by the tensile strength of the aluminum since the failure in the laminate took place on its tensile side by cracking in the aluminum layer. The large positive difference between flexural (683 MPa) and tensile strength (244 MPa) is attributed to the difference states of stress in the two tests. In the flexural test, the contribution of the outer aluminum layer predominates and gives an extraordinarily high value of strength. The tensile test wherein both LFT and aluminum are equally stressed is more representative of the whole LML response.

Short beam tests

Short beam flexure tests showed failure of the laminate due to delamination. Figure 7 shows effect of surface roughness on load versus displacement plots obtained from the short beam tests. The curve with a higher peak load corresponds to a specimen where aluminum surface was sandblasted to increase surface roughness, which in turn led to higher mechanical bonding between nylon 66 and aluminum. The surface roughness measurements by profilometer showed that sandblasting increased the mean surface roughness (R_a) from 0.4 μm to 3.2 μm. Mean surface roughness is defined as an arithmetic mean value of the roughness amplitude measured over a finite distance. The first load drop in both the plots corresponds to the appearance of an interlaminar crack. After the first drop, load increases again, which corresponds to the sample bearing some load during progression of the delaminated crack. This is followed by the final failure. Figure 8 shows the interlaminar crack in the specimen. The average value of the ILSS for sandblasted specimens was 34.4 MPa compared to that of 23.5 MPa for specimens not sandblasted. The results of the short beam tests are summarized in Table 2. Johnson reported ILSS values of E-glass fiber/polyester sheet molding compound (SMC), polyester resin based chopped strand mat (CSM), and polyester resin

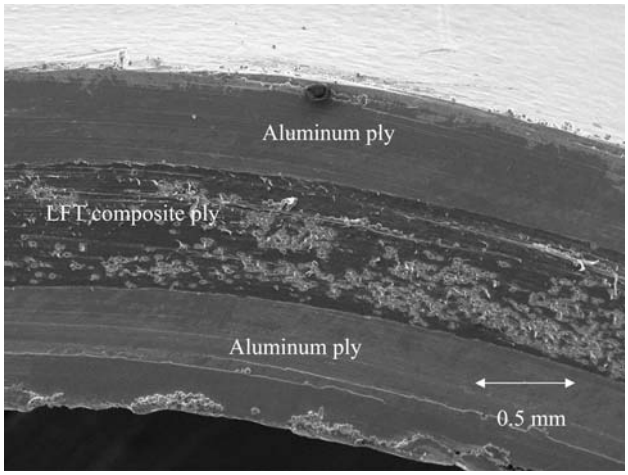

Fig. 6 Failed three-point bend test specimen of the laminate showing no delaminations between the plies

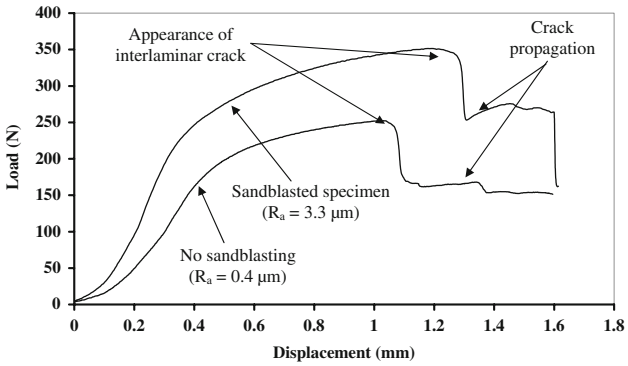

Fig. 7 Load versus displacement plots before and after sandblasting in short beam tests. Note the appearance and progression of interlaminar cracks

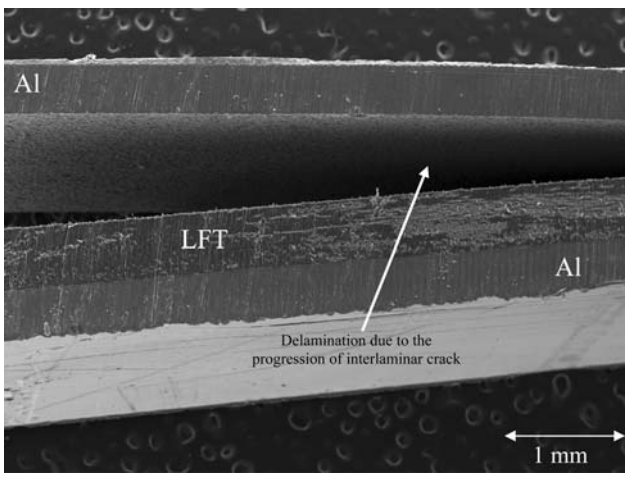

Fig. 8 SEM picture of a failed specimen in a short beam test. Note the clear interface separation between the upper aluminum and LFT layer while the interface between bottom layers is intact

Table 2 Comparison of ILSS values between no sandblasting and sandblasted specimens obtained by short beam tests

Specimen type	Average ILSS (MPa)
No sandblasting (R_a = 0.4 μm)	23.5
Sandblasted (R_a = 3.3 μm)	34.4

based woven roving composite to be in the ranges 12–20, 22–30, and 22–30 MPa, respectively [11]. Thus, the LMLs show an improvement in the ILSS over other composites.

Low-velocity impact tests

Figure 9 shows the load versus time plots for LML and LFT composite corresponding to different impact energies. The curve corresponding to low impact energy level (3 J) showed ductile behavior of the LML, Fig. 9a. The curves corresponding to 5-J impact energy showed appearance of a crack on the tensile side of the LML and LFT composite,

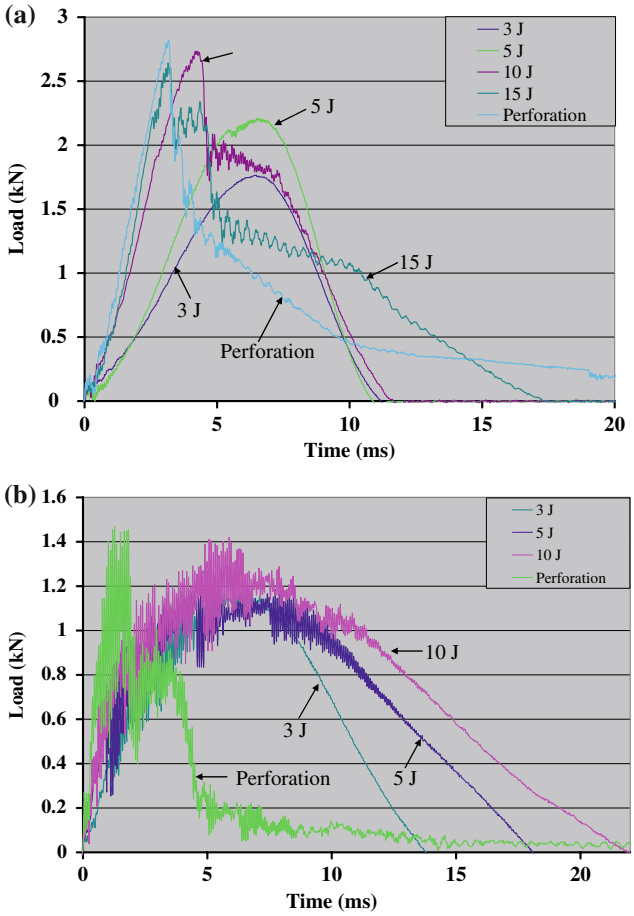

Fig. 9 Load versus time plots at different impact energy values in LVI tests. (**a**) LMLs and (**b**) LFT composites. Note that LMLs show higher peak loads at all the energy levels as compared to LFT composites

Fig. 10a. The curves at impact energy levels 10 and 15 J in the case of LMLs correspond to cracking of compressive side of aluminum ply, crack propagation, and plastic deformation of aluminum plies while in the case of LFT composite, failure was mainly due to matrix cracking and fiber/matrix debonding (Fig. 10b). When perforated, LML showed failure in the form of extensive shear fracture of top and bottom aluminum plies, delaminations between the LFT composite and aluminum plies, and fracture of the LFT composite was observed (Fig. 10c). All these failure mechanisms made LML more damage tolerant as compared to LFT composite, where fracture occurred by matrix cracking and fiber/matrix interface debonding. Specific absorbed energies corresponding to different impact energies, which were calculated by dividing absorbed energies by the respective areal densities of LML and LFT composite are shown in Table 3. Specific perforation energy was determined by dividing the perforation energy by the areal density. For LML, average value of the perforation energy was 7.58 J/(kgm^{-2}), which was significantly higher as compared to the LFT composites, 1.72 J/(kgm^{-2}).

We make a comparison of the specific perforation resistance of the LML with the values of other hybrid composites such as thermoset based FMLs (Mg/carbon-epoxy and Al/glass-epoxy with volume fraction of composites, V_c = 0.57 and 0.53, respectively) and thermoplastic based FMLs (Mg/glass-PP and Al/glass-PP with volume fraction of composites, V_c = 0.53 and 0.52, respectively) in Table 3 [17]. Volume fraction of the LFT composite in the LML was approximately 0.43. Figure 10 shows that the LML showed improved perforation resistance compared to the thermoset based FMLs, which stems mainly from the higher toughness of thermoplastics.

Conclusions

Hybrid composite laminates, consisting of layers of LFT composite and aluminum, were processed by compression molding. The laminate showed nonlinear behavior in tension and three-point bend tests. The Young's modulus of the laminate was found to be approximately 44.8 GPa and the tensile strength was approximately 244 MPa. Failure mechanisms such as delaminations between the plies, fiber breakage and pullout, plastic deformation of aluminum plies, etc. were observed. ROM calculations of the laminate properties such as density and modulus matched well with the experimental results. Three-point bend tests showed a maximum stress of approximately 683 MPa. Failure took place by cracking of the aluminum ply on the tensile side without any ply delamination. ILSS by short beam tests was found to be 34.2 MPa. Increase in interfacial roughness between LFT and Al resulted in higher ILSS. LVI

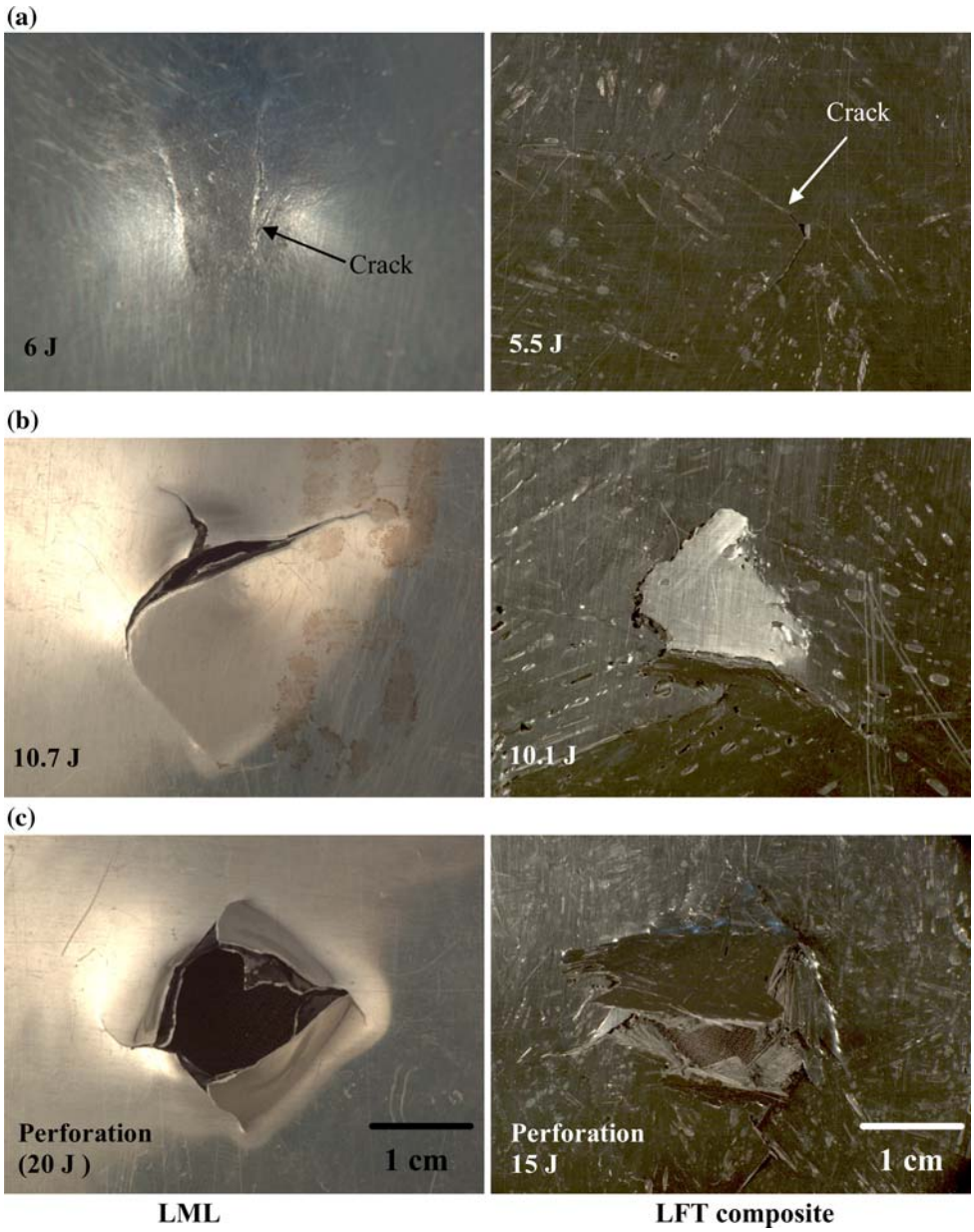

Fig. 10 Damage at various energy levels in LMLs and LFT composites. (**a**) Appearance of first crack at approximately 5 J. (**b**) Crack opening takes place at 10 J. Note that LML undergoes considerable plastic deformation. (**c**) Perforations at 20 J and 15 J in LML and LFT composite, respectively. Note extensive delaminations in LML

Table 3 Comparison of LVI test results between LFT composites and LMLs

LFT			LML		
Impact energy (J)	Specific peak load (N/kg m^{-2})	Specific absorbed energy (J/kg m^{-2})	Impact energy (J)	Specific peak load (N/kg m^{-2})	Specific absorbed energy (J/kg m^{-2})
2.80	275	0.31	3.61	741	1.03
5.47	256	0.74	5.96	892	1.85
10.1	225	1.52	10.70	993	3.51
Perforation	207	1.72	15.70	951	5.45
			Perforation	1000	7.58

LML showed significant improvement in the impact properties over the LFT composite

tests showed that the LML had significantly improved specific perforation energy (7.58 J/(kgm^{-2})) over the LFT composite (1.72 J/(kgm^{-2})). This increase in the perforation energy was mainly because of the various failure mechanisms such as ply delaminations, bending and shear fracture of aluminum plies, and fracture of LFT composite layer.

Acknowledgements Authors gratefully acknowledge the financial support from Federal Transit Administration (FTA), Contract # W911NF04-2-018. We thank Mr. Pavan Chintalapati for his help with aluminum surface preparation and Dr. Griffin for help in taking SEM pictures.

References

1. Gramann PJ, Davis BA, Rios AC (2003) Compression molding. Carl-Hanser-Verlag, Munich
2. Chawla KK (1998) Composite materials, 2nd edn. Springer-Verlag, New York
3. Vogelesang LB, Vlot A (2000) J Mater Process Technol 103:1
4. Wittenberg TC, van Baten TJ, de Boer A (2001) Aircraft Des 4:99
5. Vlot A, Gunnink JW (2001) Fiber metal laminates—An introduction. Springer, New York
6. Krishnakumar S (1994) Mater Manuf Process 9:295
7. Chawla N, Chawla KK (2006) Metal matrix composites. Springer, New York
8. Laliberte JF, Poon C, Straznicky V, Fahr A (2000) Polym Compos 21:558
9. Cortes P, Cantwell WJ (2006) Polym Compos 27:264
10. Abdullah MR, Cantwell WJ (2006) Compos Sci Technol 66:1682
11. Johnson AF (1986) Composer 17:233
12. www.quadrantcomposites.com. Accessed 15 Aug 2007
13. www.e-lft.com. Accessed 15 Aug 2007
14. Richard B, Heinrich E, Oliver G, Wenzel K, Frank H (2004) In: Int SAMPE Tech Conf 3145
15. Meyers MA, Chawla KK (1998) Mechanical behavior of materials. Prentice Hall, Upper Saddle River
16. Guillen JF, Cantwell WJ (2002) Polym Compos 23:839
17. Cortes P, Cantwell WJ (2005) Compos B 37:163